Polymer 49 (2008) 3590–3600

Contents lists available at ScienceDirect

Polymer

journal homepage: www.elsevier.com/locate/polymer

Analysis of interfacial action of rectorite/thermoplastic polyurethane nanocomposites by inverse gas chromatography and molecular simulation

Xiaoyan Ma [a,*], Xiaohong Qu [a,b], Qilu Zhang [a], Fang Chen [a]

[a] Department of Applied Chemistry, School of Science, Northwestern Polytechnical University, Xi'an 710072, China
[b] Aerospace Chemical Propulsion Factory, Xi'an 710025, China

ARTICLE INFO

Article history:
Received 1 March 2008
Received in revised form 14 April 2008
Accepted 8 May 2008
Available online 13 May 2008

Keywords:
Nanocomposites
Molecular simulation
Inverse gas chromatography

ABSTRACT

The compatibility of surface properties and the degree of interfacial action between filler and base directly affect the structure of their composites and make great contribution to a series of properties of composite materials. Interactions among rectorite (REC), quaternary ammonium salt and polymer are investigated via molecular simulation. Inverse gas chromatography (IGC) has been used to investigate the surface properties of REC, organic-modified rectorite with dodecyl benzyl dimethyl ammonium bromide (12-OREC) and hexadecyl trimethyl ammonium bromide (16-OREC), and thermoplastic polyurethane (TPUR). The correlation of the surface properties and the interfacial action between REC and TPUR and the structure of composite were analyzed. The results indicate that the modification of REC lowers its surface energy, and changes the surface from being acidic to being predominantly basic and increased the binding energy hence improving the dispersibility of 12-OREC and 16-OREC in TPUR; 12-OREC was found to be the best dispersibility in TPUR because the dispersive energy is approached to TPUR, the acid–base property is most comparable with TPUR and the binding energy between 12-OREC and TPUR is larger, which can yield higher interfacial strength.

1. Introduction

Polymer clay nanocomposites are attracting increasing interest in the area of polymer science and engineering for their good properties compared with polymers alone or conventional micro- and macro-composite materials because of its large aspect ratio [1–3]. The improvements of these new composite materials include a high static and dynamic modulus, increased tensile, flexural strength and modulus, high thermal stability, heat distortion temperature, a decrease in gas permeability and flammability, an increase in the biodegradability rate of biodegradable polymers and so forth. The morphology of composites, including dispersion and exfoliation of clay, dispersion of elastomer phase in blend systems, crystal form and size of crystallization polymer, significantly influences the various properties of nanocomposites. To take advantage of the nanosize of these clays, the challenge is to exfoliate and disperse the individual platelets within the polymer matrix which requires favorable polymer–organoclay interactions according to thermodynamic theory. An appropriate interaction among the polymer matrices, clay, and the organic surfactant used in modifying the clay is essential to obtain high levels of exfoliation. The surfactant used to modify the clay may be primary, secondary, tertiary, and quaternary alkylammonium cations or some organic cations with functional groups. Organic cations in organoclay can enlarger interlayer *d*-spacing and lower the surface energy of inorganic host, resulting in a better miscible characteristic among components. Additionally, the organic surfactant cations with functional groups can react with the polymer matrices, improving the strength of the interface between the inorganic and the polymer matrix, and support larger driving force for clay exfoliation in polymer. That means the interaction between organoclay and polymer matrices plays a key role in forming the exfoliated polymer clay nanocomposite. It is well known that polar polymer like nylon prefer to choose the organoclay made from surfactant with one long alkyl tail while the non-polar polymer like PP and PE may favorable to choose organoclay made from surfactant with two long alkyl tails, and some polymer like thermoplastic polyurethane, SAN, and PC may prefer to choose organoclay with some functional organic groups on surfactant such as hydroxyethyl. In our previous work [4,5] on clay nanocomposites, we have found that different surface properties of organoclay and polymer matrices will provide different morphologies and properties owing to their interfacial interaction. Consequently, characterization of the surface properties of both filler and polymer will be a good way to predict the performance of obtained systems. In this study, method of molecular simulation (MD) and inverse gas chromatography (IGC)

---

* Corresponding author. Tel.: +86 2988474157; fax: +86 2988491826.
E-mail address: m_xiao_yana@nwpu.edu.cn (X. Ma).

0032-3861/$ – see front matter © 2008 Elsevier Ltd. All rights reserved.
doi:10.1016/j.polymer.2008.05.006

have been employed to gain the surface properties of both clay and polymer in system of thermoplastic polyurethane/organic rectorite nanocomposites, which are synthesized in our previous work, and a relationship between surface properties of the two components and interface action in final nanocomposites was expected to be obtained.

Molecular simulation techniques are used to explore and characterize the molecular scale structure, and to predict binding energies and basal spacing of polymer/clay nanocomposites by Toth et al. [6] and Fermeglia et al. [7]. They found that the alkylammonium cations can provide functional groups that can react with the polymer to improve the strength of the interface between the inorganic component and the macromolecule. Inverse gas chromatography (IGC) has been used to investigate the surface properties of calcined kaolins and the effect on the mechanical properties of a nylon-6 composite containing the clay by Ansari and Price [8,9]. They believed that the modification of the kaolin with an aminosilane coupling agent lowered its surface energy so that it was comparable with that of the polymer matrix and changed the surface from being acidic to being predominantly basic. So the better results were achieved for the coated kaolin than the uncoated material and this correlated with the surface energy measured.

Previously, we prepared TPUR/organic rectorite nanocomposites by melt mixing using various kind of organic rectorite and found that different types of surfactants show different results on the morphology and properties of nanocomposites. Rectorite (REC) [4,5] is a kind of clay mineral with structure and characteristics much like those of montmorillonite (MMT). It is a sort of regularly interstratified clay mineral with alternate pairs of dioctahedral mica-like layer (non-expansible) and dioctahedral smectite-like layer (expansible) at ratio of 1:1 in a unit cell. Cations of Na^+, K^+ and Ca^{2+} lie in the interlayer region of 2:1 mica-like layers and 2:1 smectite-like layers, whereas the exchangeable hydrated cations reside in the latter. The hydrated cations between the smectite-like interlayers can be exchanged with cationic surfactants such as organic quaternary ammonium salt, so the REC structure can be intercalated and exfoliated, which is similar to MMT. This modified clay, with lower surface energy, will tend to be organophilic and be more compatible with polymer matrix. In order to understand the influence of surface character of organoclay on the morphology and mechanical properties of their nanocomposites, we build the structure model of REC, organic REC (OREC) with two different quaternary ammonium salts (quat), dodecyl benzyl dimethyl ammonium bromide (quat1227) and hexadecyl trimethyl ammonium bromide (quat1631), and TPUR using technique of molecular simulation, and calculate the interaction energy between REC, OREC and polymer. Also, we report IGC measurements of the surface properties of REC, OREC and TPUR to compare the compatibility of surface properties, their surface energy and acid–base properties. All the research in this article have been done to explain the effect of the surface properties and the interfacial action quantitatively and to find the insight on the relationship of surface properties and mechanical performance.

2. Experimental and modeling

2.1. Materials

Sodium rectorite [REC; Mica $(Na, Ca, K)_2(Al_4)[Si_6Al_2]_8O_{20}(OH)_4$] and smectite [$E_{0.66}$; $(Al,Mg)_4[Si,Al]_8O_{20}(OH)_4\cdot nH_2O$] were refined from clay minerals available in Wuhan, China. The CEC is 45 meq/100 g, which was tested using ammonium acetate alcohol as extractant. Polyurethane elastomer (TPUR), polyester type 5290 was provided by the Foam Plastics Factory (Tianjin, China). Two different quaternary ammonium salts (quat1227, quat1631), were obtained from Xi'an Chemical Agent Factory (Xi'an, China). Nonpolar solvents (hexane, heptane, octane and nonane) and polar solvents (chloroform, ethyl acetate, acetone, tetrahydrofuran (THF), dioxane and diethyl ether), provided by Shanghai Chemical Reagent Company of China, were used as probes. All these solvents are of analytical grade and used without further purification.

2.2. Synthesis of OREC

Sodium REC was screened with a 300-mesh sieve to remove impurities. A certain amount of screened clay was suspended in deionized water in a glass vessel using a glass rod. The quat was dissolved in prescribed amounts of water and then added to the suspended clay water solution with vigorous stirring for several minutes at room temperature. The mixture was transferred to a three-neck flask, heated to 85 °C, and stirred for 5 h. The treated products were washed and filtered repeatedly to ensure the complete removal of bromide ions; the filtrate was titrated with $AgNO_3$ until no AgBr precipitate was found. The products were then dried under vacuum at 100 °C for several hours and designated 12-OREC and 16-OREC for the modified clay with surfactant quat1227 and quat1631, respectively.

2.3. Strategy of simulation

We built the unit cell of REC crystal using the Crystal Builder modulus of the Materials Studio molecular modeling package (v.4.2, Accelrys, San Diego, CA, USA). The model structures of all quaternary ammonium were generated using the 3D sketcher tool of Materials Studio and the amorphous structures for TPUR using the polymer build tool. All structures optimized using the Universal force field with the convergence criterion being set to 4.18×10^{-4} kJ/mol.

2.4. IGC analyses

The mineral stationary phases were prepared by compacting the REC, OREC, grinding and sieving to a particle size of 180–250 μm particle size, respectively. The REC, 12-OREC, and 16-OREC stationary phases were packed into 600 mm × 3.0 mm stainless steel columns and conditioned at 150 °C under nitrogen for 24 h prior to use.

The polymer stationary phases were prepared by the support for the preparation of the chromatographic columns, diatomite was coated with TPUR solution according to the soaking method of Al-Saigh and Munk [10], then dried at room temperature to constant weight in a vacuum oven to obtain 10 wt% polymer coated based on the weight of support, and sieved to a particle size of 180–250 μm particle size. The four stationary phases were packed into 600 mm × 3.0 mm stainless steel columns and conditioned at 100 °C under nitrogen for 24 h prior to use.

IGC analyses were performed on a GC7890II gas chromatograph (Tianmei Apparatus Company in Shanghai, China) equipped with a flame ionization detector. Dried nitrogen was used as a carrier gas and flow-rates were measured using a calibrated soap bubble flowmeter. A small quantity of solvent was injected manually with a 0.1 μl Hamilton syringe. Retention times were recorded and processed by the N2000 chromatography workstation (Zhejiang University, China). Methane gas was used as a non-interacting marker to correct the dead volume in the column. Each value reported is the result of at least three elutions. The usual checks were carried out to ensure that results were recorded at infinite dilution.

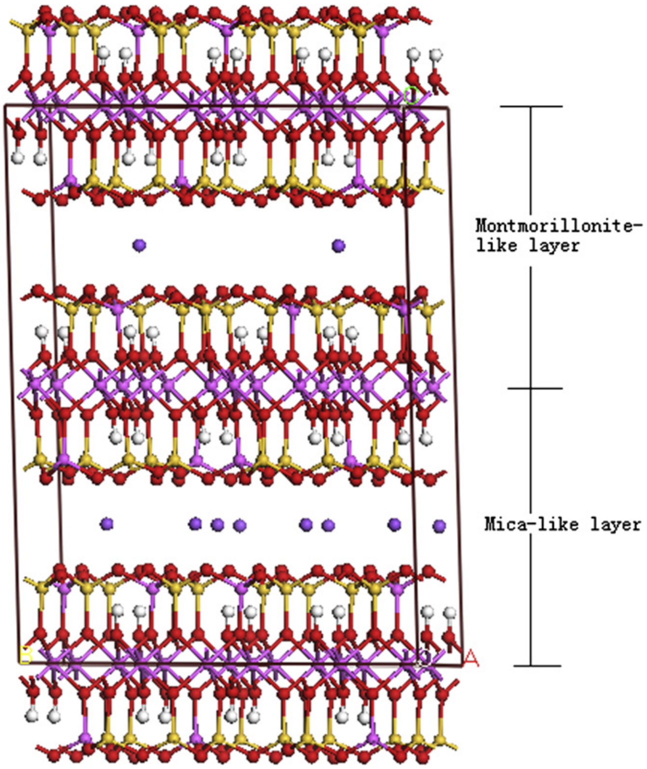

Fig. 1. Model of REC.

3. Results and discussion

3.1. The interaction energy calculated by molecular simulation

3.1.1. The models of components

Ideal chemical structural formula of rectorite has mica-like layer and montmorillonite-like layer regularly interstratified at ratio of 1:1 in a unit cell, in which the two layers' chemical formulas are [4,5]:

Mica-like layer: $(Na, Ca, K)_2(Al_4)[Si_6Al_2]_8O_{20}(OH)_4$
Montmorillonite-like layer: $(E_{0.66})(Al, Mg)_4[Si,Al]_8O_{20}(OH)_4 \cdot nH_2O$

So, in this study, corresponding crystal structure of REC model can be build through one mica layer overlapping one montmorillonite layer. The mica layer is directly employed from the Crystal Builder modulus of the Cerius2 molecular modeling package (v. 4.2, Accelrys, San Diego, CA, USA); and the montmorillonite layer is modified from the mica layer model that we adopted by substituting aluminum ions with magnesium ions. The resulting lattice is monoclinic, with space group $p1$, and characterized by the following lattice parameters: $a = 0.510$ nm, $b = 0.889$ nm, $c = 2.469$ nm, $\alpha = 90°$, $\beta = 99°$, $\gamma = 90°$. Fig. 1 shows the initial model structure of Na-REC with a supercell of $2a \times 2b \times 1c$, i.e. a model of Na-REC contains periodically replicated four unit cells; two unit cells are in x-direction, and two cells y-direction. Each cell of REC contains layers of a dioctahedral mica-like layer with eight sodium ions at the interlayer fixed and a dioctahedral montmorillonite-like layer with two sodium ions at the interlayer exchangeable. The net charge of each layer of montmorillonite-like layer is -0.66. To bring the charge neutrality in the Na-REC model, sodium ions are inserted in the interlayer clay spacing, which are not strongly fixed and can be exchanged by other cations [4,5].

Molecular mechanics were carried out in a Materials Studio modeling environment and the final model of REC is shown in Fig. 1. Fig. 2 shows the energy change of forcite geometry optimization for REC.

Two quaternary ammonium salts acted as surfactants in this study. The model structures of all quats were generated using the 3D sketcher tool of Cerius^2 and optimized using the Universal force field with the convergence criterion being set to 4.18×10^{-4} kJ/mol. Fig. 3 shows the optimized structures of quat1227 and quat1631.

The characteristic of TPUR structure contains repeated carbamate units as follow:

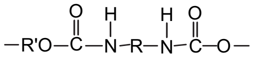

$$-R'O-\overset{\overset{\displaystyle O}{\|}}{C}-\overset{\overset{\displaystyle H}{|}}{N}-R-\overset{\overset{\displaystyle H}{|}}{N}-\overset{\overset{\displaystyle O}{\|}}{C}-O-$$

in which R represents the rigid segment and R′ the soft segment. The practical structure of TPUR performed in experiment displays a linear structure with stiff groups as well as soft chains coexist that makes simulation difficult to perform. Takeing into account the structure of practice polymer used in the experiment, we constructed the TPUR structure by predigested method. In this paper, to build the model of TUPR, R was set to be 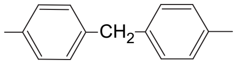 and R′ to be $-CH_2-CH_2-CH_2-CH_2-$ and the three degrees of polymerization (DP) were adopted. The amorphous structure of TPUR was constructed by three molecule of TPUR, and then subjected to an initial energy minimization using the Universal force field, with the convergence criterion being set to 4.18×10^{-4} kJ/mol. Fig. 4 shows the amorphous structures of TPUR.

3.1.2. The molecular dynamics and the interaction energy

According to the final models of REC, quaternary ammonium salts and polymer, we can build various models of different kinds of OREC as well as the OREC/TPUR composites as shown in Figs. 5 and 6(a). All systems are subjected to an energy minimization using UFF with the same convergence criterion as we did before. Here assuming that two sodium ions in silicate layers in the supercell can be exchanged, the basic space of 12-OREC and 16-OREC are 2.54 and 2.57 nm according to their WAXD data [11].

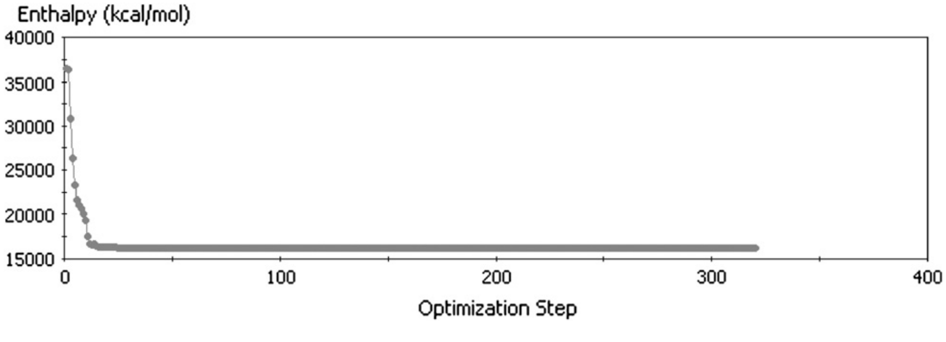

Fig. 2. The energy change of geometry optimization for REC.

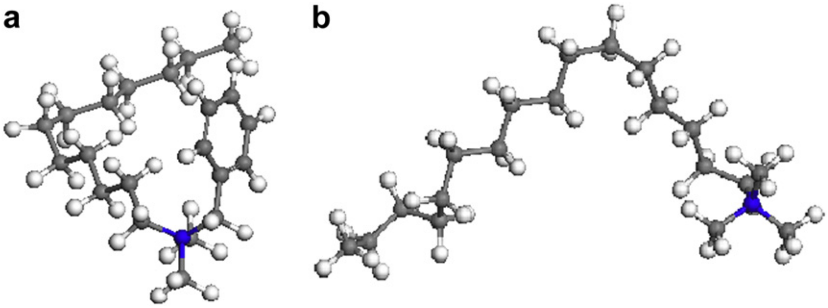

Fig. 3. The optimized models of (a) quat1227 and (b) quat1631.

After the energy minimization, molecular dynamics is started in an NVT ensemble at 600 K. The positions of the REC and sodium atoms were fixed during simulations, while the polymer molecule and the quats were kept unconstrained. Fig. 5(a) and (b) displays the final models of organoclay, 12-OREC and 16-OREC. After molecular dynamic simulation, the final models of nanocomposites were obtained as shown in Fig. 6(b). The total, potential, kinetic and non-bonded energies of the REC/TPUR, 12-OREC/TPUR and 16-OREC/TPUR versus the simulation time are reported in Fig. 7.

Each type of energy (except kinetic energy which is the function of temperature) in dynamic process for the three-nanocomposite systems, as shown in Fig. 7, decreases rapidly first and then stabilizes to an approximately constant value, indicating that every system reaches a balanceable state.

Fig. 5 shows the distribution of organic modifiers in the interlayer clay sheet in ORECs. From Fig. 5(b) we can see that after molecular dynamic simulation, the surfactant chains flatten on the clay surface and cover almost the entire surface, due to which TPUR can dock on top of the quats and reach only a small portion of the REC, i.e. the polymer molecules collapse onto the quats themselves rather than directly on the clay surface, as the quats shield the interactions between the clay and the polymer, the larger the quat volume, the larger the shielding effect the quat performs. A quat molecule has a neat positive charge, which is not restricted on the nitrogen atom but delocalizes over the entire molecule. As long as they are separated by more than the sum of their van der Waals radius, interactions between the REC oxygen and the surfactant carbon atoms are always attractive, being mainly electrostatic and secondarily van der Waals. Distribution of surfactants in this composite is consistent with the system of 12-aminolauric acid modified montmorillonite studied by Sikdar et al. [12]. However, Okamoto et al. [13–15] reported another type of distribution with modifiers crystallized between the interlayer of layered filler. This may due to the force field we adopted, which could not exactly describe the behavior of polymer crystal.

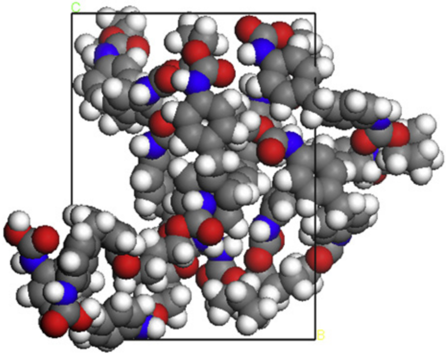

Fig. 4. The amorphous model of TPUR.

Fig. 6(a) shows the initial positions of intercalated organic modifiers and polymer in nanocomposites. The final conformation of organic modifiers and polymers in the intercalated nanocomposites after MD simulation is shown in Fig. 6(b). In the initial model, the organic modifiers are sandwiched by polymers and REC layer. From Fig. 6(b), it is evident that, although polymers and organic modifiers have changed their conformations during simulation, the polymer and REC layer are still apart with the surfactants midst, which indicates that surfactants have stronger non-bonded interactions with REC layer than the polymer.

The binding energy $E_{\mathrm{quat/REC}}$ can be calculated according to the following equations:

$$E_{\mathrm{quat/REC}} = E_{\mathrm{REC}} + E_{\mathrm{quat}} - E_{\mathrm{total}} \tag{1}$$

in which $E_{\mathrm{quat/REC}}$ is the binding energy between surfactant and REC; E_{REC} and E_{quat} represent the corresponding energy of REC and surfactant in the optimized conformation of the organoclay, and E_{total} is the total energy of the organoclay. In order to compute the binding energy between REC and surfactant, the model after molecular dynamic simulation of OREC (shown in Fig. 5(b)) should be constructed to calculate E_{total}. The corresponding energy E_{REC} was calculated from the OREC structure created from the optimized conformation of OREC by removing the surfactant molecules without further minimization, and the E_{quat} was obtained by the same way after removing all the REC platelet out from the optimized conformation of OREC. Similarly, we can get the binding energy of polymer matrix and fillers from the optimized conformation of nanocomposites. All the results of the energies for different systems are listed in Tables 1 and 2.

From Table 2 we see that combination between ORECs and TPUR is more effective than that between pure REC and TPUR with a strongest combination of 12-OREC/TPUR system. The difference between OREC/TPUR and REC/TPUR is due to the import of quaternary ammonium salts which change the character of REC surface from inorganic to organic. The strong interaction between 12-OREC and TPUR, compared with 16-OREC and TPUR, may attribute to the stronger interaction of quat1227 and REC that depicted in Table 1. So we suggested that the benzyl group of quat1227 quaternary ammonium salt is more active and take up bigger space cubage which makes quat1227 a better modifier than quat1631 does.

As rectorite is a kind of mineral clay, which is not studied much compared with MMT, the model of its chemical structure was not established. So, in this study we obtained the model arbitrarily by employing model of mica and without further validation. However, from the analysis above, we consider the model proper to some extent, though, there is still much work to be done to perfect the model.

3.2. The interaction analysis by IGC

Inverse gas chromatography (IGC) has been widely used to investigate the surface free energies of solid power or polymer.

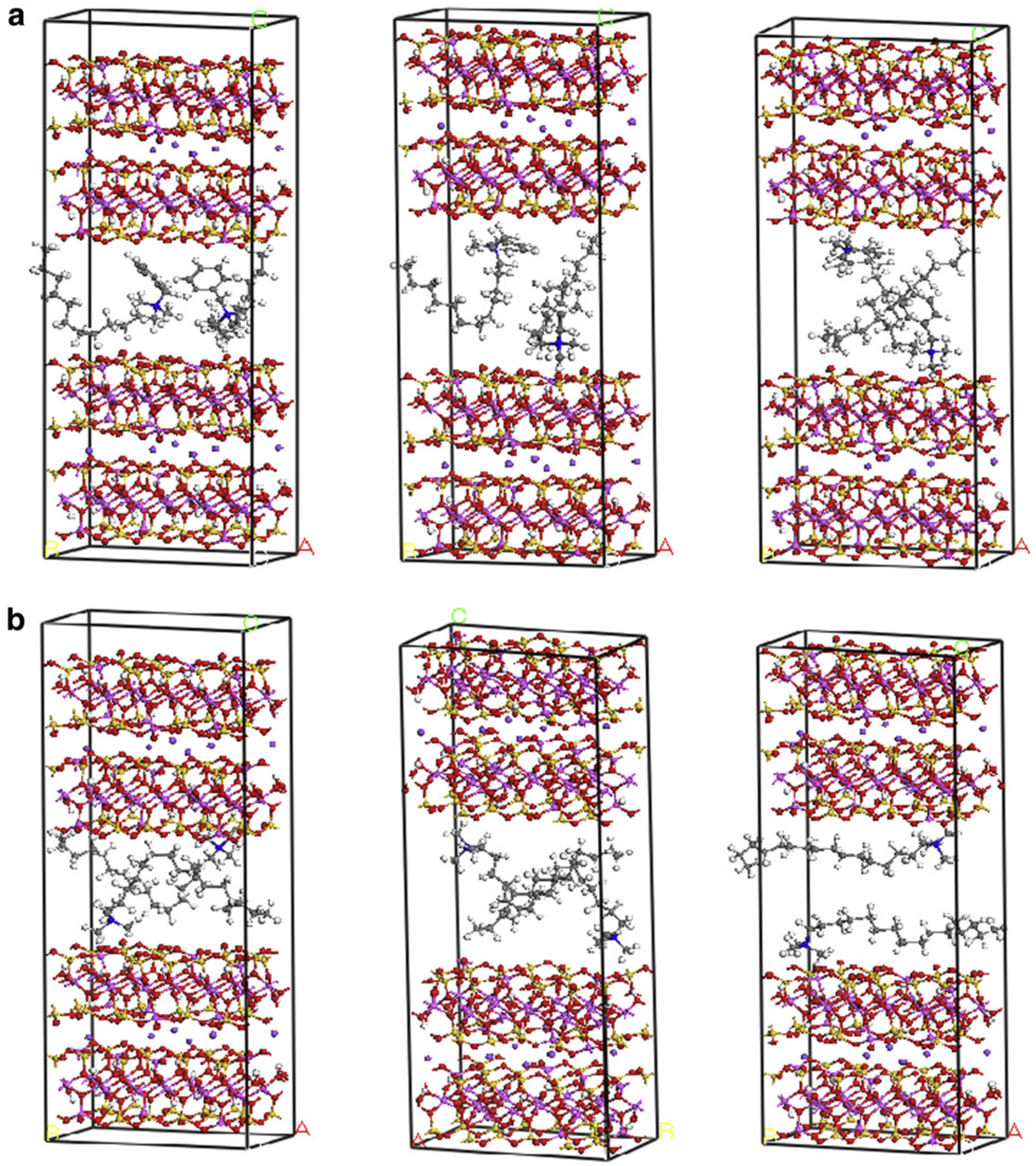

Fig. 5. (a) The initial, optimized and after-dynamic modeling structure of 12-OREC. (b) The initial, optimized and after-dynamic modeling structure of 16-OREC.

Using IGC technique, the dispersive energy and Lewis acid–base interaction of fixed phase with flow phase in column can be tested under special conditions, and the total surface energy can be written as the sum of the following two items [16],

$$\gamma_S = \gamma_S^D + \gamma_S^{SD} \tag{2}$$

where γ_S^D and γ_S^{SD} are dispersive and specific contributions, respectively. In this study, dispersive and specific contributions were characterized for all the samples using IGC method.

3.2.1. The dispersion component of surface free energy

In IGC at infinite dilution the dispersive component of the surface energy can be characterized by injecting a homologous series of *n*-alkanes into the column containing the polymer or powder.

The primary measurement in IGC is the specific retention volume, V_g, which can be calculated from the following equation [17]:

$$V_g = Fj\frac{(t_R - t_M)}{m}\left(\frac{p_0 - p_w}{p_0}\right)\left(\frac{T}{T_{\text{meter}}}\right) \tag{3}$$

where F is the carrier gas flow-rate; t_R is the retention time; t_M is the retention time of a non-adsorbing marker (air); p_0 is the outlet column pressure; p_w is the vapour pressure of water at the flow-meter temperature; T_{meter} and T are the ambient and column temperature; m is the mass of adsorbent and j is the James–Martin compressibility factor.

The free energy of adsorption ΔG_a of *n*-alkanes is given by:

$$\Delta G_a = RT \ln V_n + C \tag{4}$$

where R is the ideal gas constant, T the absolute temperature and C a constant depending on the reference state of adsorption. In the case of *n*-alkanes, ΔG_a is equal to the free energy of adsorption corresponding to dispersive interactions only.

Since ΔG_a or $RT \ln V_n$ varies linearly with the number of carbon atoms of the *n*-alkanes, it becomes possible to define an incremental value, ΔG_{CH_2}, which no longer depends on the arbitrary choice of the standard reference state of the adsorbed alkane. That is [18],

$$\Delta G_{CH_2} = -RT \ln\left(V_{g,n}/V_{g,n+1}\right) \tag{5}$$

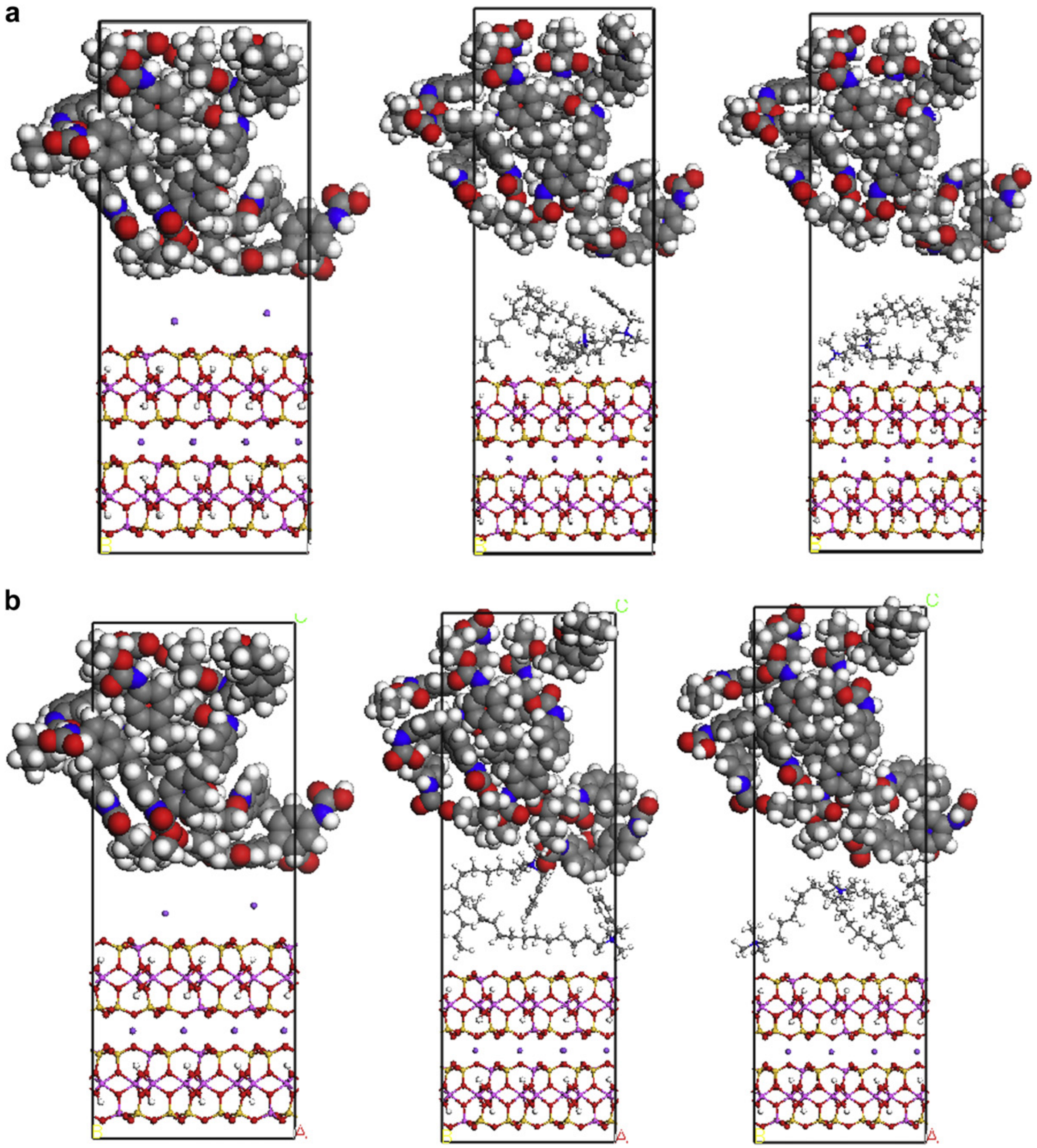

Fig. 6. Systems of REC/TPUR, 12-OREC/TPUR and 16-OREC/TPUR (a) before and (b) after molecular dynamic simulation.

thus, allowing the calculation of the dispersive component γ_S^D of the surface free energy as [16],

$$\gamma_S^D = (\Delta G_{CH_2}/Na_{CH_2})^2/(4\gamma_{CH_2}) \tag{6}$$

where $V_{g,n}$ and $V_{g,n+1}$ are the specific retention volume of alkanes having n and $n+1$ atoms of carbon, respectively; N is Avogadro's number; a_{CH_2} is the area of a –CH$_2$– group (0.06 nm^2); and γ_{CH_2}, the surface energy of a surface made of CH$_2$ groups that was calculated from the equation [16,19]:

$$\gamma_{CH_2} = 36.8 - 0.058t \tag{7}$$

As the column temperature has the relationship with the specific retention volume of alkanes, we choose different column temperature that can gain the good symmetrical and no-tailing peak. In this paper, REC was tested from 100 to 140 °C, and 12-OREC, 16-OREC and TPUR from 60 to 100 °C. The plots of $-RT \ln V_g$ versus temperature for a series of alkane probes on the materials are exemplified for the REC, 12-OREC, 16-OREC and TPUR composite and are shown in Fig. 8.

It could be seen from Fig. 8 that all the plots exhibit linear relationship within the experimental temperature range, suggesting that the equilibrium between solvents and samples had been achieved. This indicated that V_g values were amenable for thermodynamic analysis. According to Eqs. (6) and (7), theγ_S^D values of the samples can be calculated, as shown in Fig. 9.

These results indicate that surface dispersive energies of all samples decrease as the temperature increases, and surfactants used to modify REC can low surface energy of REC and the γ_S^D value of 12-OREC was most close to the value of TPUR. The γ_S^D value of REC was the highest due to its structure which is alternate pairs of dioctahedral mica-like layer (non-expansible) and dioctahedral smectite-like layer (expansible) in a 1:1 ratio, and the surface displays much hydrophilic hydroxyl group with strong activity. After

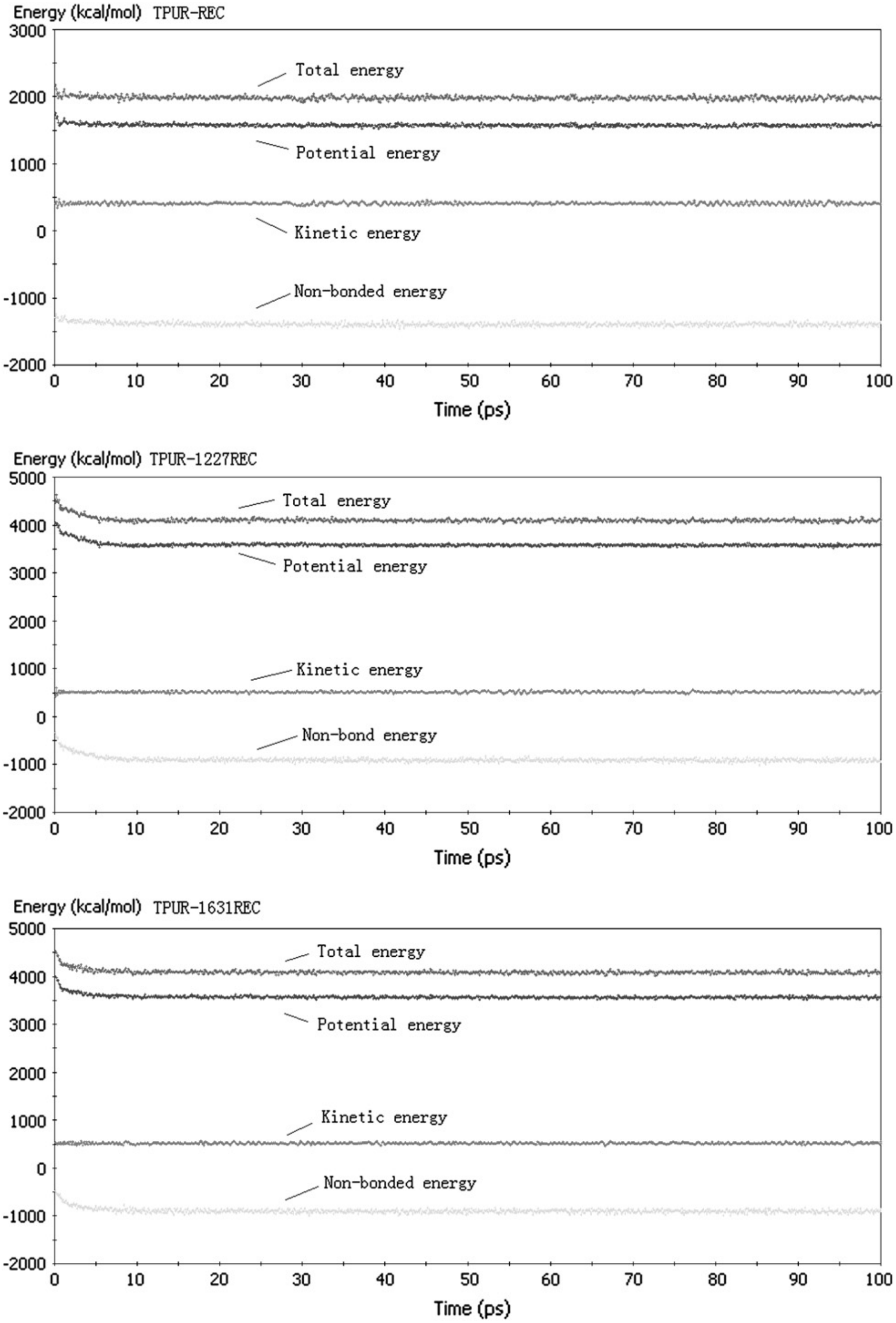

Fig. 7. Total, potential, kinetic and non-bonded energy (kcal/mol) versus time during the data collection stage for REC/TPUR, 12-OREC/TPUR and 16-OREC/TPUR systems.

modification through cation exchange reaction, the active group of REC surface was covered with long-chain quaternary ammonium salts, resulting in an enhanced hydrophobic property of 12-OREC and 16-OREC and the smaller value of γ_S^D of organoclay. Further more, we also find that the γ_S^D value of 12-OREC is lower than 16-OREC, which may result from the different structure of quaternary ammonium salts and the final conformation of their ORECs; this may attribute to the high charged benzyl group (in quat1227) [13,14].

Table 1
The interaction energy between quat and REC

Systems	Energy (kJ/mol)			
	E_{REC}	E_{quat}	E_{total}	$E_{quat/REC}$
12-OREC	1.38×10^5	1.86×10^3	1.40×10^5	314
16-OREC	1.37×10^5	1.5×10^3	1.38×10^5	291

Table 2
The interaction energy in REC/TPUR composite systems

Systems	Energy (kJ/mol)			
	E_{TPUR}	E_{REC}	E_{total}	$E_{TPUR/REC}$
REC/TPUR	11409	68663	79837	236
12-OREC/TPUR	10489	70588	79983	1093
16-OREC/TPUR	10446	71251	80717	980

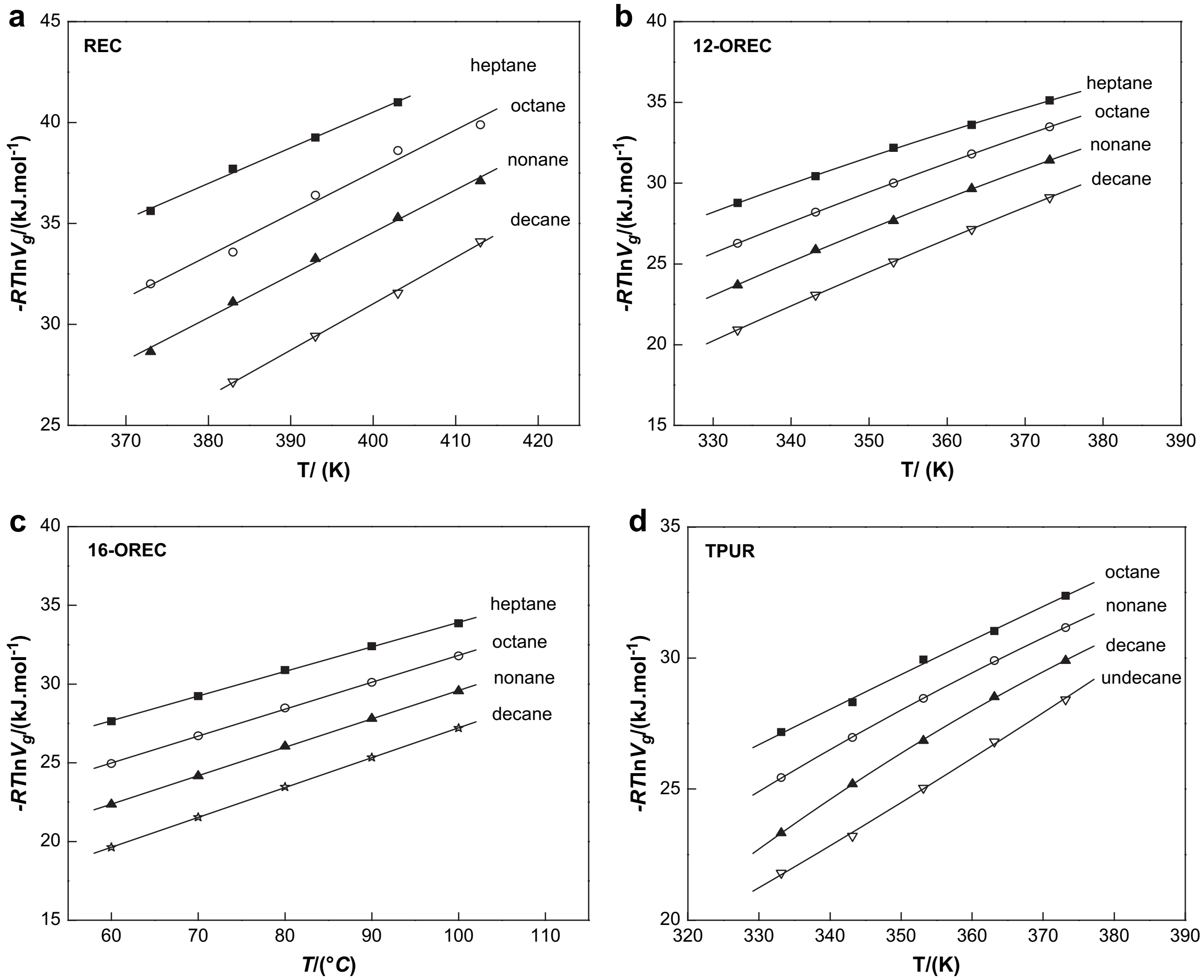

Fig. 8. Plots of $-RT \ln V_g$ versus temperature for alkane probes on (a) REC, (b) 12-OREC, (c) 16-OREC and (d) TPUR.

3.2.2. Lewis acid–base interactions

A comprehensive insight into the Lewis acid–base surface interactions can provide better understanding of the influence of the physical and mechanical properties of the nanocomposites, which is of great importance for the choice of surfactant when intended to modify the plastics with organoclay. An appropriate acid–base interaction between polymer and fillers will provide a specific intermolecular interaction within the mixture, and provide the system a better interface action, which is of great significance to design the composite and blend systems.

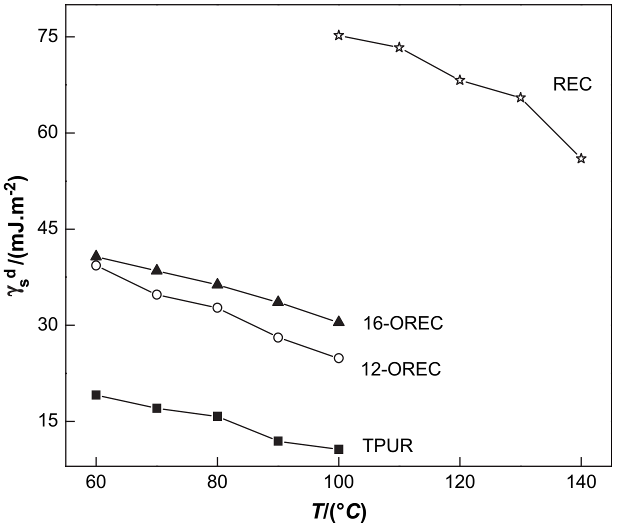

Fig. 9. Variation of the value of γ^d_{REC}, $\gamma^d_{12\text{-}OREC}$, $\gamma^d_{16\text{-}OREC}$ and γ^d_{TPUR} with temperature T of REC, 12-OREC, 16-OREC and TPUR.

According to Brookman and Sawyer, the specific interactions' contribution to the free energy of adsorption, ΔG_a^{AB}, may be described as the difference between the specific polar adsorbate and imaginary *n*-alkane that possesses the same saturated vapour pressure. ΔG_a^{AB} can be calculated from the following equation [20]:

$$-\Delta G_a^{AB} = RT \ln V_g^0 - RT \ln V_g^{ref} \qquad (8)$$

where V_g^0 is the specific retention volume of polar probe; and V_g^{ref} is the retention volume of a hypothetical alkane that possesses the same saturated vapour pressure as the corresponding polar probe. Flour and Papirer suggested that a plot of $RT \ln V_g^0$ as a function of the logarithm of saturated vapour pressure ($\lg P_0$) of the alkane probe should show a straight line, which could act as a standard. The results for the polar probes deviate from reference line to some extent. Fig. 10 displays the plots of ΔG_a^{AB} versus the logarithm of saturated vapour pressure $\lg P_0$ for REC and ORECs samples.

It is clear that chloroform, an acidic probe, exhibited significant deviations relative to the reference line for REC, 12-OREC, and 16-OREC, indicating different basic active sites on the surfaces of REC, 12-OREC and 16-OREC. On the other hand, THF, the basic

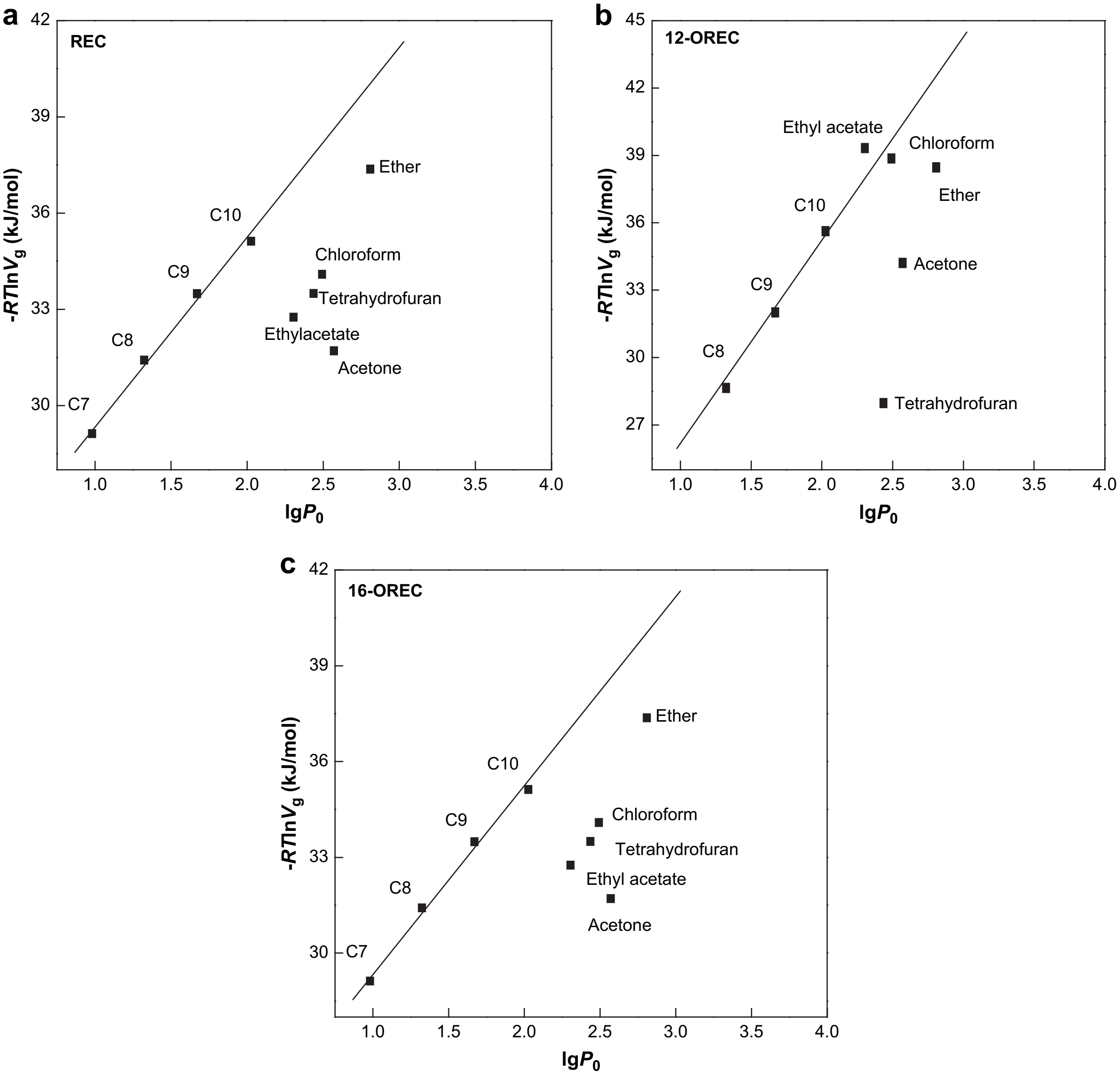

Fig. 10. Plots of $-RT \ln V_g$ versus $\lg P_0$ of polar and apolar probes on (a) REC, (b) 12-OREC, and (c) 16-OREC at 373 K.

probe, also presented a stronger specific interaction with clay and organoclays, indicating different acidic active sites on the surfaces of REC and ORECs. Moreover, the obvious deviations from the reference line were also observed for amphoteric probes, ethyl acetate and acetone, further confirming that both acidic and basic active sites are presented on REC and ORECs surface. From Fig. 10, we can also find that the deviations of different probes for REC, 12-OREC and 16-OREC from the reference line are different, indicating that the surface acidic or basic action of three kinds of REC is distinguishing.

The acid constant (K_a) and base constant (K_d), which usually describe the ability of a polymer surface to act as electron acceptor and donor, are related to the enthalpy of adsorption of the polar probe, $-\Delta H_a^{AB}$, from the following equation based on Saint and Papirer approach:

$$-\Delta H_a^{AB} = \mathrm{DN}K_a + \mathrm{AN}K_d \tag{9}$$

where DN [21] and AN [22] are the donor and acceptor values of the polar probes, respectively. $-\Delta H_a^{AB}$ can be calculated from the following equation:

$$\Delta G_a^{AB} = \Delta H_a^{AB} + \Delta S_a^{AB} T \tag{10}$$

where ΔS_a^{AB} is the entropy of adsorption of the polar probe. $-\Delta H_a^{AB}$ can be obtained from the slopes of the plots of $\Delta G_a^{AB}/T$ as a function of $1/T$. The ΔG_a^{AB} values of REC, 12-OREC and 16-OREC, TPUR at

Table 3
The measured values of adsorption energy $-\Delta G$ for the polar liquids at various temperatures (kJ/mol)

Probes	$-\Delta G_{REC}$			$-\Delta G_{12\text{-}OREC}$			$-\Delta G_{16\text{-}OREC}$			$-\Delta G_{TPUR}$		
	373 K	393 K	413 K	333 K	353 K	373 K	333 K	353 K	373 K	333 K	353 K	373 K
Chloroform	−0.49	−0.86	−1.30	4.77	4.45	4.06	8.80	8.54	7.87	–	–	–
THF	11.71	11.77	11.61	4.80	4.42	4.06	6.06	5.98	5.90	5.61	4.96	3.67
Dioxane	–	–	–	–	–	–	–	–	–	6.43	5.98	5.17

Table 4
The data of acid–base characteristics of REC, 12-OREC, 16-OREC and TPUR

Sample	K_a	K_d	K_d/K_a
REC	0.51	0.30	0.59
12-OREC	0.37	0.46	1.24
16-OREC	0.08	0.71	8.88
TPUR	0.68	0.41	0.60

Table 5
Mechanical performance of REC/TPUR, 12-OREC/TPUR and 16-OREC/TPUR

Mechanical performance	REC/TPUR		12-OREC/TPUR		16-OREC/TPUR	
	2 phr	5 phr	2 phr	5 phr	2 phr	5 phr
Tensile strength (MPa)	43.04	41.41	57.93	52.4	49.27	43
Percentage of breaking-elongation (%)	569	572	604	673	608	648
Tear strength (kN/m^2)	84.9	88.26	112.71	127.6	99.04	117.9

different temperature are summarized in Table 3. K_a and K_d could be calculated from Eq. (9), and are summarized in Table 4.

Data in Table 3 show that the acidic chloroform displays large free energy with 12-OREC and 16-OREC, indicating a larger interaction between the probe and these two organoclay, while with pure REC shows only small free energy, meaning a weak interaction between the probe and pristine REC. However, THF with strong alkalescence interacted weakly with 12-OREC and 16-OREC surface but strongly with REC. From analysis above, it indicates that the pure REC surface is predominantly acidic and, after surface modification through cation exchange reaction with quaternary ammonium salts, becomes weakly basic.

The overall acid–base character of the composites surface can be evaluated from ratio of K_d/K_a. If $K_d/K_a > 1$, the surface can be considered to be basic, meaning the surface of the clay prefers to donate electron, while $K_d/K_a < 1$, the surface can be considered to be acidic [23], indicating that the surface of the clay prefers to accept electron. From Table 4, we can see that the ratio of K_d/K_a of REC is 0.59, meaning a slightly Lewis acidic character of REC, which may be due to the abounding hydroxyl group and active oxygen on the surface of REC. The ratio of K_d/K_a of 12-OREC and 16-OREC are 1.24 and 8.88, respectively, suggesting that quaternary ammonium salt can change acidic REC to a basic one. The difference of basicity between 12-OREC and 16-OREC could attribute to the degree of covered surface of REC with long organic alkyl chains on the surfactants. In order to analyze the interaction between various clays and polymer, the interaction of TPUR with probes is also tested and the ratio of K_d/K_a is also shown in Table 4. We can find that the ratio for TPUR is 0.60, meaning an acidic nature of the TPUR surface.

3.3. *The analysis of interaction on the morphology and properties of nanocomposites*

Based on the simulation and experimental study of the conformation, surface properties and interactions of various components of composites that we investigated in this paper as well as the results previously, we can find that different surfactants can offer organoclays' different surface properties, consequently, make the nanocomposites show different morphologies and performances. So the study on the relationship between the compatibility of surface properties and the degree of interfacial action is very important.

In order to obtain the relationship between the surface property and binding energy of the filler–matrix and the morphology of their nanocomposites, we should introduce the results of Ref. [4,5], which showed a previous study on the morphologies and properties of REC/TPUR and OREC/TPURs from the surfactants quat1227, quat1631 modified TPUR in our Lab. The morphology analysis showed that REC dispersed mainly to agglomerate in the TPUR when containing 2 g REC per hundred grams resin (phr); 12-OREC dispersed better dispersion and exfoliation in the TPUR resin when content is 5 phr; 16-OREC exhibited uniform dispersion of organoclay along with little agglomerate in the TPUR matrix. It can be proposed that a closed dispersion energy of components for both filler and polymer matrix will be favorable for getting a well dispersed clay nanocomposites, i.e. the decreased dispersive energy of fillers can improve their dispersibility in low surface energy polymer TPUR and form a uniform morphology of clay polymer nanocomposites; we can get an uniform morphology of TPUR-based nanocomposite from organoclay 12-OREC since the dispersive energy of 12-OREC is close with that of TPUR. Moreover, a matched acid–base action can enhance the interaction of filler and polymer matrix, resulting in a higher interfacial strength and consequently better mechanical properties, as shown in Table 5. Weak basic properties of 12-OREC may have a good interaction with the TPUR with weak acidic surface properties, while the stronger basic surface of 16-OREC may support a weak interaction for composites of TPUR/16-OREC, and the acid surface of REC could lead to bad interfacial action; high interfacial interaction between clay and polymer may be the main reason for high mechanical properties and thermal stability, which agrees with the results of our experiments for this system. So we can conclude that 12-OREC with lower dispersive energy and matched acid–base interaction with TPUR can result in the best dispersibility clay nanocomposites and lead to higher binding energy between 12-OREC and TPUR, which can yield higher mechanical properties and higher thermal properties.

4. Conclusions

Models for REC, ORECs modified by quaternary ammonium salt, polymer TPUR, and their nanocomposites are constructed and the binding energy of clay and surfactants, organoclay and polymer was calculated through molecular simulation. It is found that the binding energy between quat1227 and REC is higher than quat1631, and so does 12-OREC and TPUR. This may attribute to the conformation of final organoclay, the largely covered surface of organoclay modified by organic long alkyl chains of surfactant can provide a favorable dispersibility of clay in polymer and can easily be intercalated by polymer, consequently, performing a uniform morphology and higher mechanical properties.

Inverse gas chromatography (IGC) has been used to investigate the surface properties of the three kinds of clay and TPUR. The results indicate that the surface dispersive energy of all samples decreased as the temperature increased, and the modification of REC with quaternary ammonium salts can low its surface energy. The γ_S^D value of 12-OREC was most close to the value of TPUR, which may be the main reason for the good dispersibility of organoclay 12-OREC in TPUR. The results of Lewis acid–base interaction showed that the ratio of K_d/K_a for REC, 12-OREC and 16-OREC is 0.59, 1.24 and 8.88, respectively, suggesting that quaternary ammonium salts can change the nature of the acidic REC to be a basic surface, and 12-OREC shows a weak basic properties, while the 16-OREC shows a strong basic properties; the weak basic properties of 12-OREC may lead to a strong interfacial interaction with weak acidic TPUR, which may directly affect the morphology of their composites and make great contribution to a series of properties of composite materials. The dispersive energy of the pristine REC is much higher than the TPUR, and both of them are acidic, so the interface action is weak and REC dispersed badly in the TPUR resin, which agrees with the result of the binding energy between REC and TPUR calculated by molecular simulation as well as the experimental results reported previously. The dispersion energy of REC is greatly decreased by modification of quat1227 and quat1631, and surfaces of 12-OREC and 16-OREC change from acid to base, which improved the dispersibility of 12-OREC and 16-OREC in TPUR matrix and resulted in a high binding energy between organoclay and polymer TPUR; 12-OREC was found to have the best dispersibility in TPUR because the dispersive energy of 12-OREC is most close to TPUR, and the acid–base property is most comparable with TPUR, which can also be proved from the binding energy between 12-OREC and TPUR from the molecular simulation; the matched properties of dispersive energy and Lewis acid–base interaction for filler and polymer matrix can yield higher interfacial strength and good performance for their composites.

Acknowledgements

This study was supported by National Science Foundation of China (20674062) and New Century Excellent Talents in University (NCET-06-0880).

References

[1] Cui LL, Ma XY, Paul DR. Polymer 2007;48(21):6325–39.
[2] Jeon K, Lumata L, Tokumoto T, Steven E, Brooks J, Alamo RG. Polymer 2007; 48(16):4751–64.
[3] Dennis HR, Hunter DL, Chang D, Kim S, White JL, Cho JW, et al. Polymer 2001; 42(23):9513–22.
[4] Ma XY, Liang GZ, Lu HJ, Huang Y. J Appl Polym Sci 2005;97(5):1907–14.
[5] Ma XY, Lu HJ, Liang GZ, Yan HX. Acta Polym Sin 2004;(1)::88–92.
[6] Toth R, Coslanich A, Ferrone M, Fermeglia M, Pricl S, Miertus S. Polymer 2004; 45(23):8075–83.
[7] Fermeglia M, Ferrone M, Pricl S. Fluid Phase Equilib 2003;212(1–2):315–29.
[8] Ansari DM, Price GJ. Polymer 2004;45(6):1823–31.
[9] Ansari DM, Price GJ. Polymer 2004;45(11):3663–70.
[10] Al-Saigh ZY, Munk P. Macromolecules 1984;17(4):803–9.
[11] Ma XY, Lu HJ, Liang GZ, Yan HX. J Appl Polym Sci 2004;93(2):608–14.
[12] Sikdar D, Katti DR, Katti KS. Langmuir 2006;22(18):7738–47.
[13] Yoshida O, Okamoto M. Macromol Rapid Commun 2006;27:751–7.
[14] Saito T, Okamoto M, Hiroi R, Yamamoto M, Shiroi T. Macromol Mater Eng 2006;291:1367–74.
[15] Saito T, Okamoto M, Hiroi R, Yamamoto M, Shiroi T. Polymer 2007;48(14): 4143–51.
[16] Dorris GM, Gray DG. J Colloid Interface Sci 1979;71(1):93–106.
[17] Conder JR, Young CL. Physicochemical measurement by gas chromatography. New York: Wiley; 1979.
[18] Zeki Y, Saigh AL. Polymer 1999;40(12):3479–85.
[19] Papirer E, Schaltz J, Turchi C. Eur Polym J 1984;20(12):1155–8.
[20] Flour CS, Papirer E. J Colloid Interface Sci 1983;91(1):69–75.
[21] Gutmann V. The donor–acceptor approach to molecular interactions. New York: Plenum; 1978. p. 17–33.
[22] Riddle FL, Fowkes FM. J Am Chem Soc 1990;112(9):3259–64.
[23] Zou QC, Zhang SL, Tang QQ. J Chromatogr A 2006;1110(1–2):140–5.